chemosensors

MDPI

Review

Advances on Sensors Based on Carbon Nanotubes

Luca Camilli [1,*] and Maurizio Passacantando [2,*]

[1] DTU Nanotech, Technical University of Denmark, DK-2800 Kongens Lyngby, Denmark
[2] Department of Physical and Chemical Sciences, CNR-SPIN, University of L'Aquila, Via Vetoio, 67100 L'Aquila, Italy
* Correspondence: lcam@nanotech.dtu.dk (L.C.); maurizio.passacantando@aquila.infn.it (M.P.)

Received: 8 November 2018; Accepted: 30 November 2018; Published: 6 December 2018

Abstract: Carbon nanotubes have been attracting considerable interest among material scientists, physicists, chemists, and engineers for almost 30 years. Owing to their high aspect ratio, coupled with remarkable mechanical, electronic, and thermal properties, carbon nanotubes have found application in diverse fields. In this review, we will cover the work on carbon nanotubes used for sensing applications. In particular, we will see examples where carbon nanotubes act as main players in devices sensing biomolecules, gas, light or pressure changes. Furthermore, we will discuss how to improve the performance of carbon nanotube-based sensors after proper modification.

Keywords: carbon nanotubes; gas sensors; bio-sensors; photo-sensors; photodetectors; pressure sensors; field effect transistor

1. Introduction

Carbon nanotubes (CNTs) can be thought of as hollow cylinders made of carbon atoms with sp^2 hybridization. In other words, they can be seen as rolled-up graphitic layers—or graphene layers. If it is only one layer—i.e., only one cylinder—then they are called single-wall CNTs (SWCNTs), whereas if there are more layers—i.e., more concentric cylinders—these are multi-wall CNTs (MWCNTs). Since the seminal paper by Iijima in 1991 [1], CNTs have been attracting a great deal of attention among material scientists, physicists, chemists and engineers because of their peculiar properties. For instance, although they are made of the same element—i.e., carbon—and have similar dimension and aspect ratio, CNTs can be either metallic or semiconducting depending on the way the graphitic layer is rolled up [2]. From a chemical point of view, CNTs' high aspect ratio makes them suitable for functionalization through chemical [3–8] or physical methods [9–12]. The high aspect ratio makes them also interesting for sensing application [13–18] as well as water filtration [19–22], because of the high surface area they can provide.

Arc-discharge is the technique that was first used to produce carbon nanotubes [23–25]. However, the yield is quite poor, as many other carbon compounds are usually also produced during the process. Therefore, a laborious work of product recovery and purification is needed after the growth. Laser ablation has also been used, where a metal-doped graphite target is hit by a high-power laser. The synthesized CNTs are often single-wall CNTs of high quality [26–28]. However it requires the use of expensive instruments, like lasers, and cannot therefore be easily scaled up. Chemical vapor deposition is the technique that is mostly used to grow CNTs. Single-wall [29–33] as well as multi-wall [34,35] CNTs can be produced, and this method has the advantage to be scalable, to allow large-area deposition and to provide CNTs that are already attached onto a substrate, hence easy to be collected. The use of external metal catalyst is often required, although CNTs have also been grown directly on stainless steel [36] or on semiconductors [37,38] without the addition of external metal.

Today, CNTs are employed for many applications, encompassing the field of reinforcement [39,40] electronics [41–43], optoelectronics [44–46], sensors [13–18], batteries [47,48] and supercapacitors [49].

In this review, we will focus on distinguished studies that have provided notable contribution to the field of carbon nanotubes for sensing applications. In particular, we will overview the works on carbon nanotube-based gas sensors, biosensors, photo-sensors, and pressure sensors (Figure 1). As there are many outstanding studies in this topic, it was impossible to discuss them all; thus, we apologize for any possible omission.

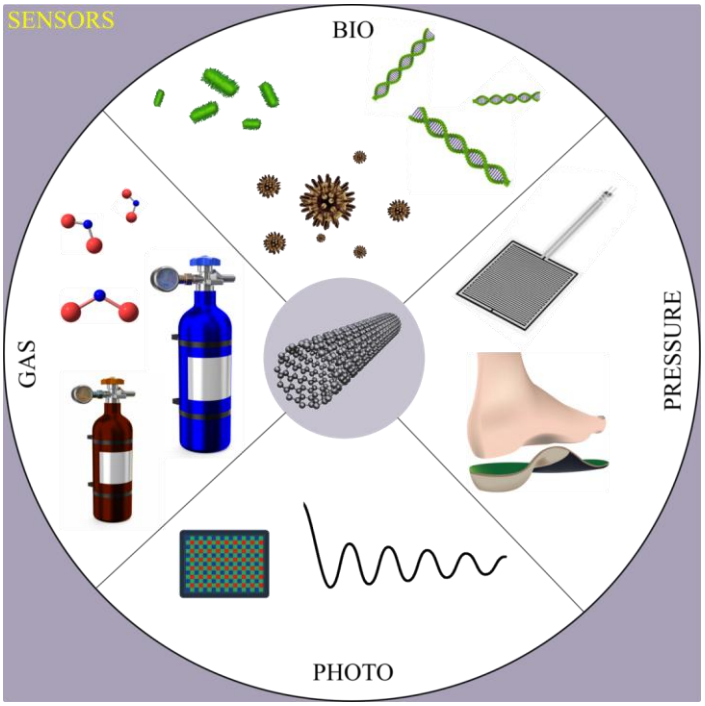

Figure 1. Carbon nanotubes have been used for a number of different applications. When it comes to sensing devices, they have been used to realize gas sensors, biosensors, pressure sensors and photodetectors.

2. Carbon Nanotube-Based Gas Sensors

Upon interaction with molecules, a charge transfer occurs between CNTs and molecules that can drastically alter CNTs' electrical conductivity. Gas sensors working with CNTs being in contact with two metal electrodes rely precisely on this phenomenon. In 2000, Kong et al. [18] demonstrated for instance that a single semiconducting SWCNT increases or decreases its conductance when exposed to NO_2 or NH_3 gas respectively (Figure 2a). The sensor exhibits a fast response (down to below 1 min) that can be attributed to the high surface area of the CNT. However the most remarkable feature is probably the fact that it works at room temperature. Metal oxides have often been used for sensing NO_2 or NH_3, however they need to work at temperatures above 200 °C in order to achieve enough sensitivity [50]. The sensor proposed by Kong et al. [18] instead operates at room temperature with sensitivity as high as 10^3, while it can recover in one hour upon annealing at 200 °C or in 12 h if left at room temperature under flow of pure argon. The high surface area, which grants CNT-based sensor a fast response, is probably also the cause of their slow recovery. In addition to annealing the sensor at high temperatures, another strategy to improve its recovery time is to illuminate it with ultra-violet (UV) radiation [14].

Still in the year 2000, Collins and coworkers [51] demonstrated that SWCNTs are also extremely sensitive to oxygen. They measured changes in both the electrical resistance and thermoelectric power when the oxygen partial pressure in gas environments was changed as low as 10^{-8} to 10^{-10} Torr. The authors also measured the change in terms of electronic density of states of the CNTs deposited on gold upon exposure to oxygen or pure argon gas through scanning tunneling spectroscopy experiments. Notably, they show that semiconducting CNTs become metallic upon oxygen exposure. Furthermore,

the authors also find that not all the SWCNTs are sensitive to oxygen, and that argon, helium or nitrogen have no noticeable doping effects on them.

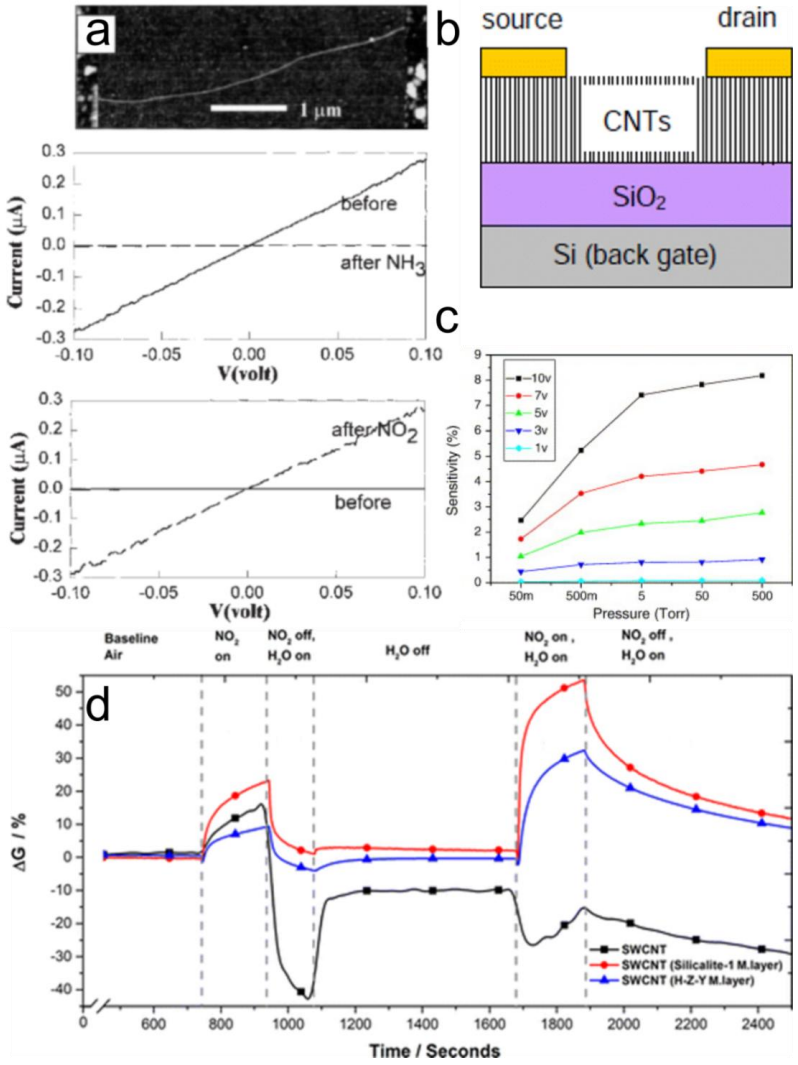

Figure 2. (**a**) Atomic force microscopy image of an individual semiconducting SWCNT bridging two metal contacts; and its current versus voltage curves collected before and after exposure to NH_3 or to NO_2. Modified from Ref. [18]. with permission from American Association for the Advancement of Science (AAAS) (**b**) Schematic of a three-terminal gas sensor with silicon substrate as back gate and a film of vertically aligned carbon nanotubes working as a channel. (**c**) The sensitivities of the device in (**b**) as a function of N_2-filling pressure at various source-drain bias voltages from 1 to 10 V without any gate voltage. Reprinted from Ref. [52] with permission from Elsevier. (**d**) Plot of the change in conductance at room temperature (ΔG) upon exposure to various combinations of NO_2 and H_2O for a blank SWCNT, a SWCNT sensor with a Silicalite-1 mixed layer and a SWCNT sensor with a hydrophilic zeolite-Y mixed layer. The first region displays the baseline conductance for each sensor type while operating in dry synthetic air, whereas in the second region, 10 ppm of NO_2 is additionally introduced to the testing chamber. The next region contains the desorption step in which the NO_2 pulse is turned off and H_2O is turned on resulting in a relative humidity of 75% inside the testing chamber, aiding NO_2 desorption from the sensor surface. In the subsequent region, H_2O is turned off to return the relative humidity of the chamber to 0% and recover baseline conductance. Next the sensors are exposed to 10 ppm of NO_2 while operating at 75% chamber humidity. Finally, in the last region of the graph, the NO_2 is turned off and relative humidity is set at 75% for the desorption cycle. Reprinted with permission from Ref. [53]. Copyright (2016) American Chemical Society.

Nevertheless, in 2005, Huang et al. [52] showed that, with a three-terminal device based on multi-wall CNTs, N_2 can indeed be detected. In this work, two metal electrodes (i.e., source and drain) are placed on a film of vertically-aligned multi-wall CNTs that is deposited on a Si/SiO_2 substrate, with Si acting as back gate (Figure 2b). The authors found that the sensitivity towards N_2 increased when applying a high source-drain bias voltage (Figure 2c). Moreover, since the device is more sensitive when a negative gate voltage is applied, it was concluded that a change of free holes concentration in the CNTs film played the major mechanism for the N_2 gas detection.

Regarding other inert gases, for instance hydrogen, it was found that palladium-modified CNTs can detect it down to 100 ppm concentrations [54].

In general, sensors based on metal-decorated CNTs are more sensitive than those based on pristine CNTs for a wide range of gases and vapors [55–58]. Combining CNTs with other materials in a composite device sensor can be useful not only to improve the CNT's intrinsic sensitivity, but to improve other characteristics as well.

One issue with CNT-based sensors is for instance the low selectivity to specific gases or vapors. In case a CNT sensor is exposed to both NO_2 and water, the signal coming for the detection of the latter could mask the detection of the former. This is due to the fact that while NO_2 adsorption onto CNTs' walls tends to increase the electrical conductivity, water induces an opposite response (i.e., decrease in electrical conductivity). To mitigate this issue, Evans et al. [53] have recently combined CNTs with zeolites. While bare CNTs are unable to detect NO_2 in humid conditions, due to the aforementioned issue, CNTs coupled with highly hydrophilic zeolites successfully detect it. The reason is because the zeolites trap water molecules before these can actually reach the CNTs, which therefore only sense NO_2 (Figure 2d).

Instead of building a sensor where the CNTs sensing features (for instance, the sensitivity or the selectivity) are improved by combination with other materials (i.e., metal nanoparticles, or zeolites, as we have seen above), an alternative concept is to improve common metal oxide sensors by combination with CNTs. As mentioned earlier, metal oxide sensors need temperatures of at least 200 °C in order to function properly. This, in turn, means that such devices consume a lot of energy. However, recent studies performed in the last decade have shown that sensors combining metal oxides with CNTs can indeed operate at lower temperatures, even down to room temperature. In 2004, for instance, Wei et al. [59] fabricated a hybrid SnO_2/CNT sensor by spin coating and then thermal treating an organometallic solution with single-wall CNTs dispersed in it. By comparing the results from a hybrid device with the ones from a SnO_2-only device, the authors unambiguously demonstrated that the hybrid device is almost two orders of magnitude more sensitive at room temperature for the detection of NO_2.

Espinosa and coworkers [60] reported that also multi-wall CNTs if added to a metal oxide sensor would lead to a remarkable improvement of its sensing properties. In particular, they added oxygen-functionalized MWCNTs to three different types of metal oxides, namely SnO_2, WO_3 or TiO_2. The authors concluded that these sensors are more sensitive toward NO_2 down to the ppb range at room temperature, and can fully regenerate after the exposure to the pollutant gas. More interestingly, their results also show that there should be an optimum amount of CNTs to be added to each specific metal oxide material in order to enhance the sensitivity.

The last two examples clearly point out how the sensing performance of a standard metal oxide sensor can be improved by simply including CNTs into the device.

Very recently, Nguyet et al. [61] found that when CNTs are mixed with SnO_2 nanowires, instead of SnO_2 film like in Ref. [59] or SnO_2 powders as in Ref. [60], the hybrid sensor can reach an ultralow detection limit of about 0.68 ppt. The sensors consisted of a film of multi-wall CNTs bridging between a bare Pt-electrode and a Pt-electrode with pre-grown SnO_2 nanowires (Figure 3). The device operated in the reverse bias mode and the main gas-sensing mechanism was found to be the modulation of the leakage current due to the trap-assisted tunneling of SnO_2 nanowires through the adsorption of

NO_2 gas molecules. Most likely, the ultralow detection limit of this hybrid sensor can be ascribed to a combination of the high surface area of both the CNT and SnO_2 nanowires.

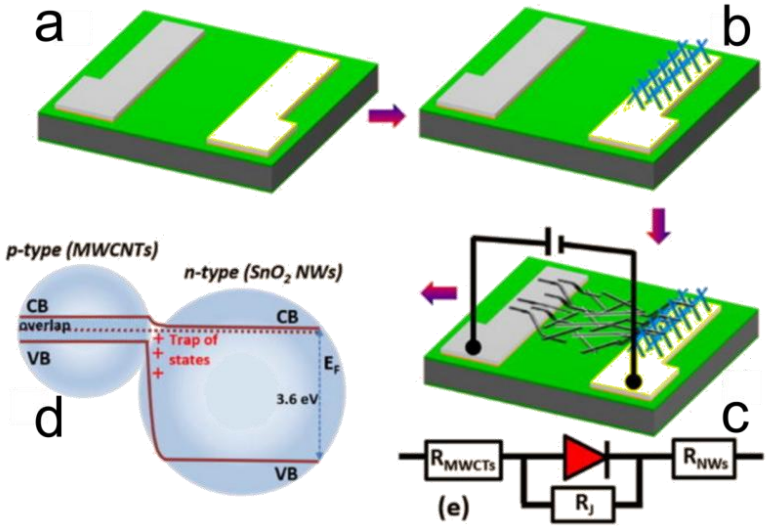

Figure 3. Scheme for fabrication of the hybrid heterojunction of MWCNTs and SnO_2 nanowires (NWs): (**a**) a pair of Pt-electrodes, (**b**) selective growth of SnO_2 NWs, (**c**) the deposition of MWNCTs to form the heterojunction, (**d**) band diagram of the heterojunctions, and (**e**) equivalent electronic. Reprinted from Ref. [61], with the permission of AIP Publishing.

3. Carbon Nanotube-Based Biosensors with FET Configuration

Bare CNTs do not exhibit compelling affinity towards biological molecules, so prior to using CNTs in biosensors they need to be functionalized with bioreceptors, such as proteins, oligo- or polynucleotides or even microorganisms and whole biological tissues [62]. These have obvious affinity with biological molecules, so they act as the sensitive element; whereas CNTs act as transducers, by collecting and converting the signal, due to the interaction between the sensitive element and the biological species to be detected, in a more detectable physical signal. Depending on the nature of this physical signal (i.e., electrical current, optical absorbance, acoustic signal, heat and so on) and, therefore, on the way it is measured, different CNT-based biosensors exist [62]. Here, we will focus on CNT-based biosensors operating with a field-effect transistor configuration (CNT-bioFET) because of their superior performance and the wide spread use.

The working principle of CNT-bioFETs is similar to that of the CNT gas sensors, which are discussed in a previous section above. Notably, when the target biological molecule interacts with the functionalized CNT, the CNT's electrical conductance changes and the target molecule is thus detected. It is worth noting that because of the functionalization, CNT-based biosensors can be highly specific towards a particular target molecule (which in general is not the case for CNT-based gas sensors). As shown in Figure 4a, for instance, only CNTs functionalized with an antibody receptor that is specific to the target biological molecule—a virus, in the example illustrated in the figure below—can successfully interact and hence detect such target molecule [63]. It follows that the bioreceptor used to functionalize the CNTs will also dictate the size of the detected biological species, which can range from small molecules like sugars, proteins, or DNA fragments to more complex systems like virus and bacteria to even cells and small fragments of tissues.

However, these conceptually-simple sensors may still suffer from non-specific binding, especially in the case of protein binding detection. Nevertheless, as we have seen already for the gas sensors, also the specificity of CNT-biosensor can be improved if the CNTs are combined with another material into a composite system. Here, it is worth noting that CNTs are not the sensing element, but owing to their high aspect ratio, high electrical conductivity and mechanical flexibility, they enable the realization of ultra-thin sensing devices with high specific surface area and fast response time.

Star et al. [64] avoided the issue with non-specific binding by coating the CNT-based sensor with a mixture of hydrophilic polymers. These polymers will then attach to biotin molecules that in turn bind specifically to the target streptavidin molecules. In addition to improving the specificity of the sensor, the polymer coating is used also to link the molecular receptor (i.e., biotin) to the sidewalls of the CNTs without the need of covalent functionalization, which would have the disadvantage of impairing CNTs' physical properties.

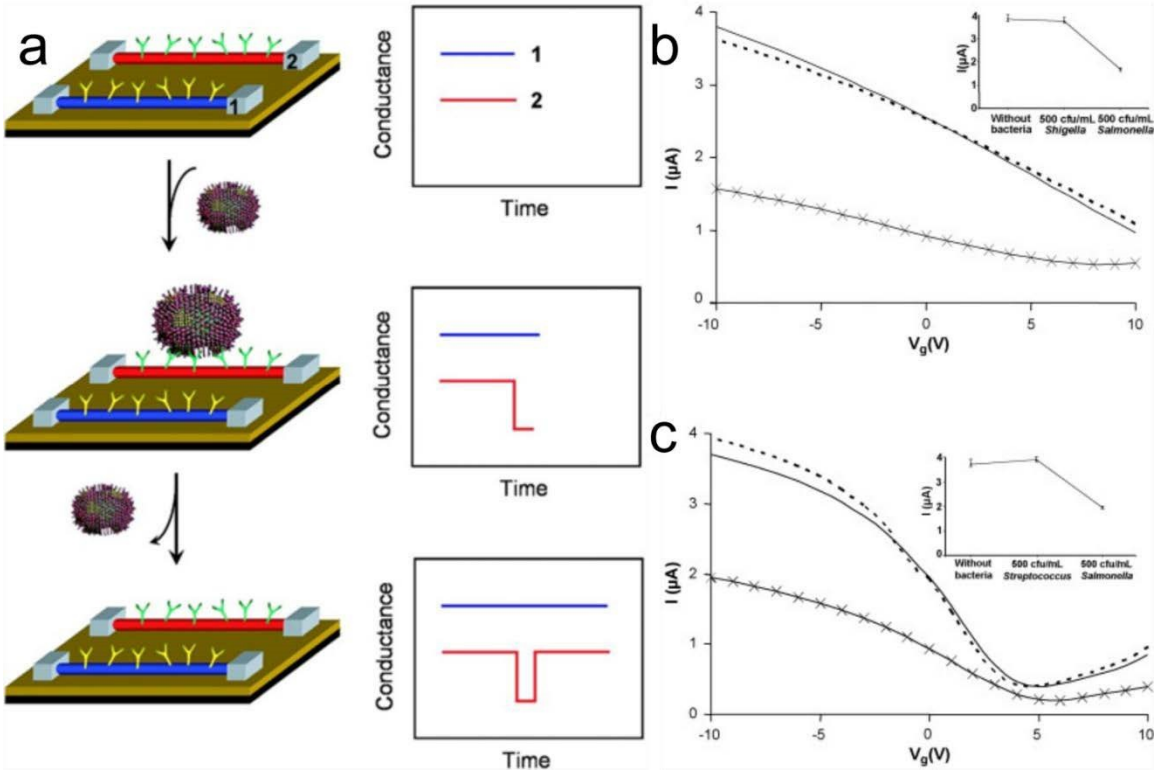

Figure 4. (**a**) Schematic illustration of the working principle of a CNT-based biosensors operating with a field-effect transistor configuration (CNT-bioFET). Only the CNT that are functionalized with the antibody receptor specific to the target virus can detect it, by producing a conductance change. The conductance can be restored when the virus unbinds from the surface. Reprinted from Ref. [63]. Copyright (2004) National Academy of Sciences. (**b**) Gate voltage dependence of the source-drain current of a functionalized CNT-bioFET before exposure to the bacteria (—) and after exposure to 500 cfu/mL of *Shigella sonnei* (- - - -) and 500 cfu/mL of *Shigella Infantis* (×). (**c**) Gate voltage dependence of the source-drain current of a functionalized CNT-bioFET before exposure to the bacteria (—) and after exposure to 500 cfu/mL of S. pyogenes (- - - -) and 500 cfu/mL of S. Infantis (×). Each electrical current plotted corresponds to the mean value of three replicates. The inset shows the behavior of the source-drain current at gate voltage = −10 V. The error bars correspond to the range of the electrical current measured for the three replicates. Reprinted form Ref. [65] with permission from Elsevier.

A similar stratagem to increase specificity was adopted by Villamizar et al. [65], who coated the CNT-bioFETs with Tween 20. Sensing studies were performed with three different and potentially competing bacteria, namely *Salmonella infantis*, *Streptococcus pyogenes,* and *Shigella sonnei*. In particular, to test whether the presence of *Streptococcus pyogenes* or *Shigella sonnei* would influence the detection of the target *Salmonella*, the biosensors were immersed in a solution containing *Streptococcus pyogenes* (or *Shigella sonnei*) and then rinsed and dried prior to being immersed in the solution containing *Salmonella*. Results clearly show that neither *Streptococcus* nor *Shigella* interfered with the detection of the target bacteria (Figure 4b,c).

CNT-based biosensors with this configuration have also been used to monitor biological reactions. For instance, Star et al. [66] used it to follow the enzymatic degradation of starch. Investigating the biodegradation of starch is useful because it has been recently introduced as filler into composite materials in order to increase the degradation rate of synthetic polymers. In Ref. [66], the authors firstly deposit starch onto CNT-bioFET, and register the consequent shift in conductance. Next, starch is biodegraded into soluble glucose upon reaction with amyloglucosidase enzyme, and can therefore be washed off by rinsing the device in water. After this process, the conductance of the CNT-bioFET recovers to a value similar to the one of the pristine device, before starch was deposited; hence indicating that starch had been indeed degraded.

One of the major limitations of CNT-bioFETs is perhaps the presence of background noise of electrostatic origin. In CNT-bioFET, the signal to be detected is in the millivolt-scale range, but this background noise causes electrostatic fluctuation in the same scale range, ultimately limiting the performance of the sensing device. The origin of such noise was not clear until recently, when Sharf and coworkers [67] performed a systematic experimental and theoretical investigation in the framework of the charge noise model. They found that the noise is generated mainly by substrate interactions and surface adsorbates, and if these contributes are removed the power spectral density of background voltage fluctuations can be reduced by 19-fold.

4. Carbon Nanotube-Based Photo-Sensors

When a photon hits a semiconducting CNT, if its energy is higher than the band gap of the CNT, an electron/hole pair is generated within the nanostructure. A built-in potential could then separate the two charge carriers so that a photocurrent can be measured. This is the concept behind a simple single-CNT photosensor.

To create the built-in potential, it is necessary to form a junction. This junction can either be of a p-n type, or a Schottky type (Figure 5a,b). In the first case, one can form a p-n junction within a nanotube electrostatically [68,69], or by chemical doping [70]. However, both approaches are technically rather challenging. Selectively doping only part of a CNT is obviously a tremendous task. On the other hand, to realize a p-n junction electrostatically within an individual CNT, one needs to define two electrodes (i.e., the two gates) that are usually less than half a micron apart. Besides, the system requires now multiple drive voltages (i.e., it is a four-terminal device, instead of a standard three-terminal one, due to the presence of a split-gate). Creating a Schottky junction is instead much easier, and is achieved by contacting a semiconducting CNT with a metal electrode of different work function [71]. If the same metal is used at both ends of the CNT, a photodetector with two symmetric Schottky barriers will be formed. These symmetric barriers lead to a reduced sensitivity because the separated charge carriers need to tunnel through another barrier before being collected. Moreover, as the sensor detects the difference of the signal intensity between two contacts, the overall performance is very poor. On the other hand, if two different metals are used to contact the two CNT ends, two different Schottky barriers will be formed and the photoresponse results in being highly enhanced (Figure 5c–e) [71,72].

In addition to devices made up of individual CNTs, also photodetectors based on CNT films can be realized [73]. However, the presence of both metallic and semiconducting tubes usually limits the overall device performance. To overcome this issue, Liu et al. [74] have recently fabricated an infrared (IR) photodetector where only highly purified semiconducting CNTs have been used. CNTs are very promising for IR detection because their absorption coefficient is one order of magnitude higher than that of traditional IR bulk materials [75]. In the devices proposed by Liu et al. [74], photovoltage is used as signal instead of photocurrent, as commonly reported. This allows improving significantly the signal-to-noise ratio because (i) shot noise and $1/f$ noise are suppressed, and (ii) the signal can be multiplied by introducing virtual contacts. With a device that operates at room temperature and zero-bias condition, the authors demonstrated detectivity of over 10^{11} Jones, broadband response from 785 to 2100 nm, and exceptional temperature and temporal stability. This, coupled to the use of a

scalable solution-based fabrication method, makes CNT-based IR photodetectors highly competitive against the traditional bulk IR detectors, such as Ge, Si, InGaAs and HgCdTe [76–78].

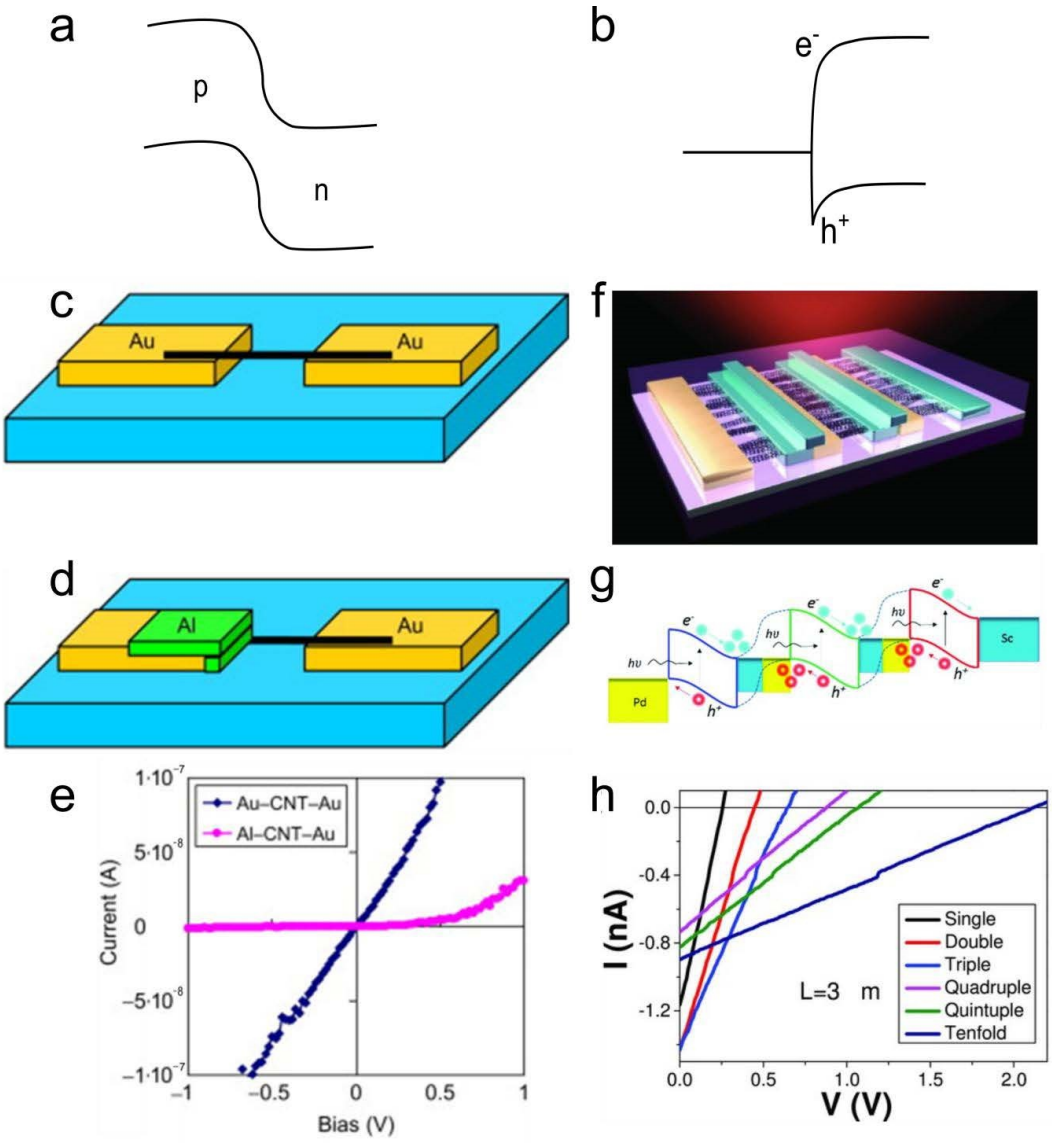

Figure 5. (**a**,**b**) Sketch of a p-n junction (**a**) and a Schottky junction (**b**). (**c**–**e**) Fabrication process of Au–CNT–Au (**c**) and Al–CNT–Au (**d**) photodiodes using a single CNT; and their I–V characteristics (**e**). (**c**–**e**) Modified from Ref. [71]. (**f**–**h**) Schematic structure of the cascade photovoltaic module consisting of $N = 3$ cells connected in series with two virtual contacts (**f**); corresponding energy band diagram illustrating the excitation and carrier accumulation process under light illumination (**g**); and corresponding I–V characteristics of the tandem cells with $N = 1$ (black), 2 (red), 3 (blue), 4 (pink), 5 (green), and 10 (Navy blue) individual cell in series during the measurements (**h**). Devices were measured under an incident power of 5.78 W cm^{-2} with $\lambda = 1800$ nm. Reproduced from Ref. [74] with permission from Wiley.

Another common configuration for CNT-based photodetectors is obtained when a CNT film is placed on a doped Si substrate to create a heterojunction. Here, the contacts can be either placed both on top of the CNT film or located one on top of the film and the second one at the bottom of the Si slab. In the former case, the collected signal will come mainly from the CNT film; in the latter case, instead, both the signal coming from CNTs and that from Si are collected, and the resulting overall signal is highly enhanced. The advantage of this hybrid photosensor when compared to a Si photosensor is

that the CNTs extend the device detection range into both the near-IR and near-UV regions of the electromagnetic spectrum [46].

Although single-wall CNTs are usually employed for the realization of these photodetectors, due to their well-defined opto-electronic properties, some groups have investigated also devices made of multi-wall tubes [79–81]. Notably, in one of our experimental works we have shown that highly defective multi-wall CNTs exhibit larger photocurrent than less defective ones [44]. Although truly intriguing, this finding still needs to be fully understood, and further experimental and theoretical studies are highly desirable.

Several groups have shown that the photoresponse in CNT-based photo-devices can be improved when the CNTs are functionalized with other nanostructures. In particular, they have been decorated with either semiconducting [8,82,83] or metal nanoparticles [84,85]. In the former case, the semiconducting material can be for instance TiO_2 or CdS. The enhancement in this hybrid system is ascribed to the charge transfer occurring between the semiconductor nanoparticle and the CNTs (Figure 6a). Once an excited electron is generated in the nanoparticle after absorption of a photon with energy larger than the nanoparticle bandgap, it can be transferred to the CNT and thus contribute to the overall electrical signal. In this case, the enhancement is due to the absorption of photons at a particular energy by the semiconducting nanoparticle. In the case of metal nanoparticles, instead, the enhancement of the photocurrent is due to the strong plasmonic local field that they generate on the CNTs (Figure 6b,c). Thus, this enhancement is not localized at a given wavelength, but it occurs in the whole spectrum where CNT are sensitive.

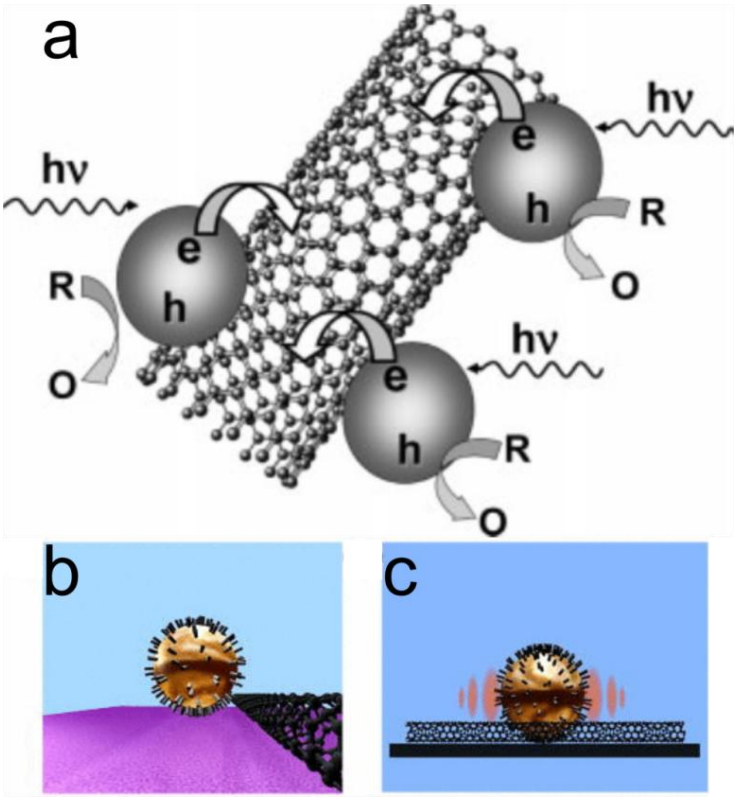

Figure 6. (**a**) Charge-transfer interaction between photoexcited CdS nanoparticles and SWCNTs. Reprinted with permission from Ref. [8]. (**b**,**c**) Principle of field enhancement on CNT due to Au nanoparticle. Structural diagrams showing (**b**) Au particle side-contacts a CNT and (**c**) plasmon coupling between Au nanoparticle and CNT when the polarization of the incident light is parallel to the CNT axis. Adapted with permission from Ref. [85].

5. Carbon Nanotube-Based Pressure Sensors

In the last decade, there has been a growing interest in the field of flexible and stretchable electronics among scientists and engineers. Notably, wearable and skin-mountable strain sensor devices are particularly intriguing due to their potential in, for instance, personalized health-monitoring, human motion detection, soft robotics and prosthetic solutions. Owing to their excellent mechanical properties [86], high mobility and current density [87], CNTs might be the ideal building blocks for such devices.

An example of personalized health-monitoring application of CNT-based sensors was suggested by Gerlach et al. [88] They designed a low-cost plantar pressure sensor that was tested inside a running shoe during walking. The sensor is a composite made of multi-wall CNTs and a polymer, i.e., polydimethylsiloxane (PDMS), and has the function of detecting unhealthy rollover patterns that could lead to pressure ulcers, which are not only a problem to individual's health but also the cause of enormous costs for the public health care system.

Another example was proposed by Park et al. [89], who realized a sensor capable of monitoring human breathing flows and voice vibrations. The sensor consists of two CNT/PDMS composite sides with a microdome array facing each other. The sensing mechanism is based on a giant tunneling piezoresistivity. Notably, the tunneling current percolating among the CNTs has high sensitivity (15.1 kPa1, with 0.2 Pa minimum detection) and rapid response (0.04 s) to pressures.

Early this year, for instance, Nela et al. [90] demonstrated a large-area high-performance flexible pressure sensor built on an active matrix of 16 $\times$ 16 carbon nanotube thin-film transistors (CNT TFTs). The CNT TFTs, acting as pixels in the sensing device, are fabricated on a polyimide film, and then covered by a commercially available pressure-sensitive rubber. The pressure-sensitive rubber has a high electrical resistance when no pressure is applied (>30 MΩ), which abruptly becomes very low when pressed (<0.1 Ω). This change in the resistance of the rubber turns on the TFTs. At a gate bias of -3 V, the ratio between the source-drain current at ON or OFF state (that is, pressed and released states, respectively) is above 10^4. The response of the device (measured as the time when source-drain current drops to 10% or reaches 90% of the current at ON state) is less than 30 milliseconds, that is much faster than human skin. Additionally, they demonstrated that the flexible pressure sensor can operate on both flat and curved surfaces without compromising its sensing accuracy (Figure 7). The main advantages of using CNTs for this particular application instead of competing materials such as organic polymers and semiconductor nanowires are higher mobility and current density, environmental stability, and superior mechanical properties.

Instead of using flat films of CNTs for fabricating pressure sensors, an alternative design consists of using bulky, three-dimensional assembly of CNTs. An example of these structures is represented by the so-called CNT sponges, which are made of long and entangled CNTs forming a random skeleton with open pores [91]. Following this idea, in 2013 we investigated the evolution of the electrical conductivity of a CNT sponge upon compression. For the experiment, two flat metal electrodes were located at the top and bottom of the CNT sponge, and the same electrodes were used to apply compression to the whole system. The electrical conductivity linearly increased with the applied compression, and increased of about 615% at compressive strains as high as 75%, resulting in a sensitivity of 1.15. Moreover, the initial value of electrical conductivity is restored once the applied load is released. A second experiment was also performed, where the contact resistance and the electrode distance are kept unaltered so as to make negligible their contribution to the change in conductivity. Notably, the CNT sponge was fixed on a rigid support in a scanning electron microscope and the compression was applied by a nano-tweezer in a confined area located at the center of the sample, far away from the fixed metal electrodes. Furthermore, this experiment confirmed the linear dependence of the electrical conductivity with the applied compression.

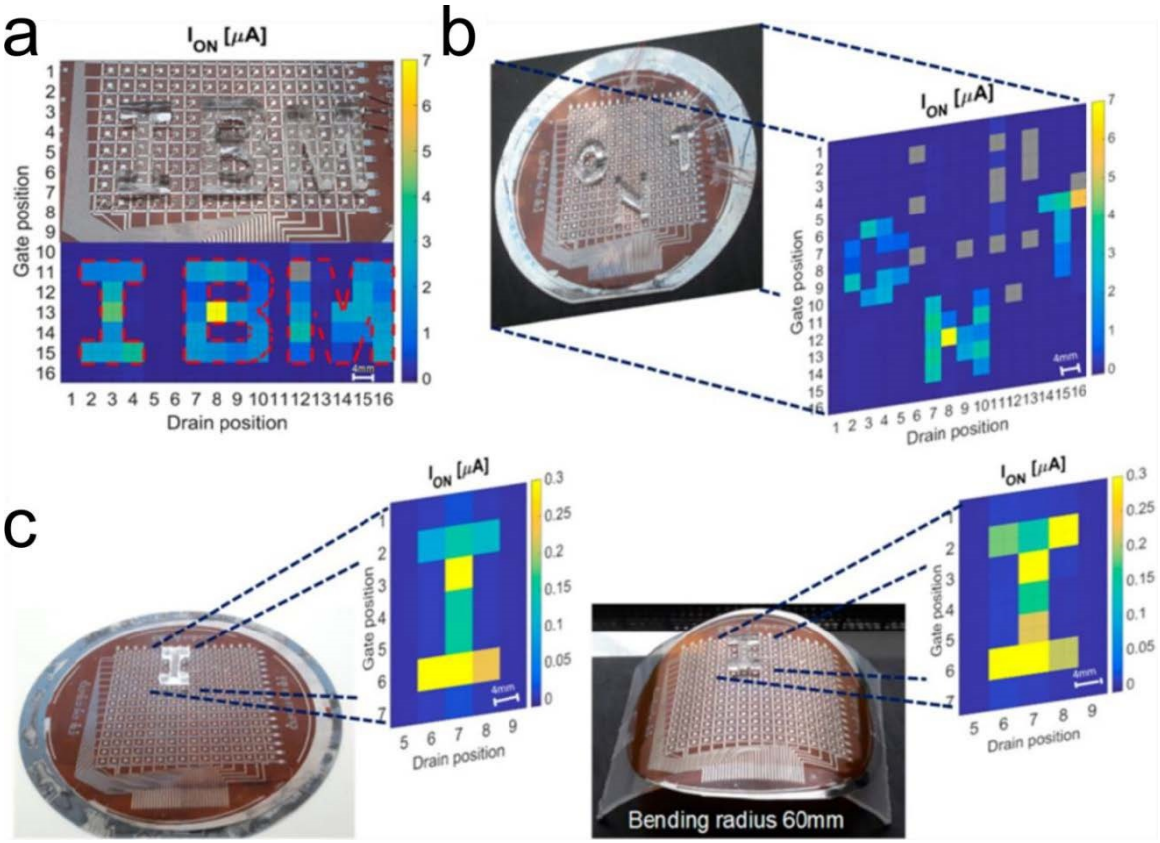

Figure 7. Pressure mapping of complex objects on flat and curved surfaces. (**a**) Current mapping of the CNT thin-film transistors active matrix showing the pressure sensing of "IBM" logo made by polydimethylsiloxane (PDMS) polymer. (**b**) Current mapping for the pressure sensing of word "CNT" made by PDMS. The defective pixels are labeled in gray color. (**c**) Comparison of pressure sensing on flat (left) and curved (right) surfaces with a bending radius of 60 mm. In both mappings, the pressure applied is 6.8 kPa. Reprinted from Ref. [90]. Copyright (2018) American Chemical Society.

This behavior is ascribed to a growing number of contact points among adjacent CNTs during compression that creates new percolating pathways for charge carriers. Thus, when a pressure is applied to the CNT sponge, the inter-tube pores are squeezed and the CNT sponge becomes denser, and eventually more CNTs touch each other. Once the compressive load is released, the sponge elastically recovers its original shape and consequently the initial number of tube contacts, so that also the electrical conductivity regains its starting value as well.

6. Conclusions, Challenges and Future Perspectives

Owing to their superior mechanical, electric and opto-electronic properties, coupled with a high aspect ratio, CNTs have been attracting a great deal of interest in many sensing applications. In this review, we have discussed concepts, design, working principle and showed a few examples of CNT-based gas sensors, biosensors, light sensors, and pressure sensors. Before concluding our work, we now summarize the major challenges that these devices need to face in order to be able to reach the market.

As of today, gas sensors are probably the most studied CNT-based sensor device, and many gases and vapors can indeed be detected. Since the realization of the first CNT gas sensors [18], the superiority of these devices compared to traditional semiconductor gas sensors was clear. While the former can work at room temperature, the latter needs high temperatures, and thus requires more energy. The major limitation of CNT gas sensors is however the lack of selectivity. We have seen in this review that this issue can be mitigated by realizing composites, where CNTs are coupled to

other materials like for instance zeolites [52]. Nevertheless, lack of selectivity is still a major roadblock hampering further spreading of these CNT devices. More work in this direction is therefore necessary. A possible path to follow in order to increase selectivity could be to use a method based on the analysis of desorption rate at elevated temperatures, as suggested for graphene NO_2 sensors, although the use of high temperature would lead to higher power consumption [92].

Several types of CNT biosensors have been reported, and here we have reviewed the ones working with a field-effect transistor configuration. In these devices, CNTs are functionalized with biomaterials specific to the target biomolecule that has to be detected. This functionalization solves the selectivity issue that we instead described for the case of CNT gas sensors. Owing to their high surface area, and the fact that they are made of carbon, CNTs are rather easily functionalized. This, coupled to recent advances in enhancing the signal-to-noise ratio [67], makes CNT biosensors very competitive, with feasibility for miniaturization. Their major drawback is probably the intrinsic risk to human and environmental health posed by CNTs [93,94]. This problem could however be mitigated if for instance CNTs are well anchored to a substrate.

CNT photodetectors are very promising, especially the ones working in the near-IR and IR range since CNT's absorption coefficient is one order of magnitude higher than that of traditional IR bulk materials [75]. Moreover, traditional IR sensors usually require sophisticated and expansive growth methods such as molecular beam epitaxial (MBE) or metal organic chemical vapor deposition (MOCVD) [95]. One of the limitations with CNT based photodetectors is that high performance requires the use of only semiconducting CNTs of high purity. This means that once CNTs are synthesized, they need a further purification and sorting step. Although these purification protocols have now become very effective and it is possible to separate metallic CNTs from semiconducting ones [96–99], the overall fabrication process becomes longer and more expensive. This issue will need to be addressed in the future so as to allow further development of CNT photodetectors.

Many advances have been done in the field of CNT-based pressure sensors, and although a higher quality and durability is still required for these devices, some of them printed on plastics exhibit already high performance [90].

In conclusion, although CNTs have been around for little less than thirty years, they still keep attracting great interest in the scientific community. Worldwide, CNTs production capacity currently exceeds several thousand tons per year. CNT are already incorporated in several commercial products, such as rechargeable batteries, automotive parts, sporting goods, and water filters [100]. Regarding CNT-based sensors, some of them, like the pressure sensors, are already at a level in which they can be commercialized; other types of sensors need instead to address some issues before they can be competitive against current technology. Nevertheless, we are confident that this class of CNT-based devices will be very important in our future every-day life.

Author Contributions: The manuscript was designed and written through contributions of all authors. All authors have given approval to the final version of the manuscript.

Funding: L.C. acknowledges funding by the Young Investigator Program of Villum Fonden, project No. 19130.

Conflicts of Interest: The authors declare no competing financial interest.

References

1. Iijima, S. Helical microtubules of graphitic carbon. *Nature* **1991**, *354*, 56–58. [CrossRef]
2. Saito, R.; Dresselhaus, G.; Dresselhaus, M.S. *Physical Properties of Carbon Nanotubes*; World Scientific: Singapore, 1998.
3. Georgakilas, V.; Kordatos, K.; Prato, M.; Guldi, D.M.; Holzinger, M.; Hirsch, A. Organic functionalization of carbon nanotubes. *J. Am. Chem. Soc.* **2002**, *124*, 760–761. [CrossRef] [PubMed]
4. Balasubramanian, K.; Burghard, M. Chemically functionalized carbon nanotubes. *Small* **2005**, *1*, 180–192. [CrossRef] [PubMed]

5. Holzinger, M.; Vostrowsky, O.; Hirsch, A.; Hennrich, F.; Kappes, M.; Weiss, R.; Jellen, F. Sidewall functionalization of carbon nanotubes. *Angew. Chem. Int. Ed.* **2001**, *40*, 4002–4005. [CrossRef]
6. Hirsch, A. Functionalization of single-walled carbon nanotubes. *Angew. Chem. Int. Ed.* **2002**, *41*, 1853–1859. [CrossRef]
7. Dyke, C.A.; Tour, J.M. Covalent functionalization of single-walled carbon nanotubes for materials applications. *J. Phys. Chem. A* **2004**, *108*, 11151–11159. [CrossRef]
8. Robel, I.; Bunker, B.A.; Kamat, P.V. Single-Walled Carbon Nanotube–CdS Nanocomposites as Light-Harvesting Assemblies: Photoinduced Charge-Transfer Interactions. *Adv. Mater.* **2005**, *17*, 2458–2463. [CrossRef]
9. Scarselli, M.; Camilli, L.; Castrucci, P.; Nanni, F.; Del Gobbo, S.; Gautron, E.; Lefrant, S.; De Crescenzi, M. In situ formation of noble metal nanoparticles on multiwalled carbon nanotubes and its implication in metal–nanotube interactions. *Carbon* **2012**, *50*, 875–884. [CrossRef]
10. Ren, G.; Xing, Y. Deposition of metallic nanoparticles on carbon nanotubes via a fast evaporation process. *Nanotechnology* **2006**, *17*, 5596. [CrossRef]
11. Scarselli, M.; Castrucci, P.; Camilli, L.; Del Gobbo, S.; Casciardi, S.; Tombolini, F.; Gatto, E.; Venanzi, M.; De Crescenzi, M. Influence of Cu nanoparticle size on the photo-electrochemical response from Cu–multiwall carbon nanotube composites. *Nanotechnology* **2010**, *22*, 035701. [CrossRef]
12. Espinosa, E.; Ionescu, R.; Bittencourt, C.; Felten, A.; Erni, R.; Van Tendeloo, G.; Pireaux, J.-J.; Llobet, E. Metal-decorated multi-wall carbon nanotubes for low temperature gas sensing. *Thin Solid Films* **2007**, *515*, 8322–8327. [CrossRef]
13. Ghosh, S.; Sood, A.; Kumar, N. Carbon nanotube flow sensors. *Science* **2003**, *299*, 1042–1044. [CrossRef] [PubMed]
14. Li, J.; Lu, Y.; Ye, Q.; Cinke, M.; Han, J.; Meyyappan, M. Carbon nanotube sensors for gas and organic vapor detection. *Nano Lett.* **2003**, *3*, 929–933. [CrossRef]
15. Tang, X.; Bansaruntip, S.; Nakayama, N.; Yenilmez, E.; Chang, Y.-L.; Wang, Q. Carbon nanotube DNA sensor and sensing mechanism. *Nano Lett.* **2006**, *6*, 1632–1636. [CrossRef] [PubMed]
16. Modi, A.; Koratkar, N.; Lass, E.; Wei, B.; Ajayan, P.M. Miniaturized gas ionization sensors using carbon nanotubes. *Nature* **2003**, *424*, 171–174. [CrossRef] [PubMed]
17. Lipomi, D.J.; Vosgueritchian, M.; Tee, B.C.; Hellstrom, S.L.; Lee, J.A.; Fox, C.H.; Bao, Z. Skin-like pressure and strain sensors based on transparent elastic films of carbon nanotubes. *Nat. Nanotechnol.* **2011**, *6*, 788–792. [CrossRef] [PubMed]
18. Kong, J.; Franklin, N.R.; Zhou, C.; Chapline, M.G.; Peng, S.; Cho, K.; Dai, H. Nanotube molecular wires as chemical sensors. *Science* **2000**, *287*, 622–625. [CrossRef] [PubMed]
19. Srivastava, A.; Srivastava, O.; Talapatra, S.; Vajtai, R.; Ajayan, P. Carbon nanotube filters. *Nat. Mater.* **2004**, *3*, 610–614. [CrossRef] [PubMed]
20. Brady-Estévez, A.S.; Kang, S.; Elimelech, M. A single-walled-carbon-nanotube filter for removal of viral and bacterial pathogens. *Small* **2008**, *4*, 481–484. [CrossRef] [PubMed]
21. Das, R.; Ali, M.E.; Hamid, S.B.A.; Ramakrishna, S.; Chowdhury, Z.Z. Carbon nanotube membranes for water purification: A bright future in water desalination. *Desalination* **2014**, *336*, 97–109. [CrossRef]
22. Camilli, L.; Pisani, C.; Gautron, E.; Scarselli, M.; Castrucci, P.; D'Orazio, F.; Passacantando, M.; Moscone, D.; De Crescenzi, M. A three-dimensional carbon nanotube network for water treatment. *Nanotechnology* **2014**, *25*, 065701. [CrossRef] [PubMed]
23. Ebbesen, T.; Ajayan, P. Large-scale synthesis of carbon nanotubes. *Nature* **1992**, *358*, 220–222. [CrossRef]
24. Ando, Y.; Iijima, S. Preparation of carbon nanotubes by arc-discharge evaporation. *Jpn. J. Appl. Phys.* **1993**, *32*, L107. [CrossRef]
25. Bethune, D.; Kiang, C.H.; De Vries, M.; Gorman, G.; Savoy, R.; Vazquez, J.; Beyers, R. Cobalt-catalysed growth of carbon nanotubes with single-atomic-layer walls. *Nature* **1993**, *363*, 605–607.
26. Guo, T.; Nikolaev, P.; Thess, A.; Colbert, D.T.; Smalley, R.E. Catalytic growth of single-walled manotubes by laser vaporization. *Chem. Phys. Lett.* **1995**, *243*, 49–54. [CrossRef]
27. Yudasaka, M.; Komatsu, T.; Ichihashi, T.; Iijima, S. Single-wall carbon nanotube formation by laser ablation using double-targets of carbon and metal. *Chem. Phys. Lett.* **1997**, *278*, 102–106. [CrossRef]

28. Maser, W.; Munoz, E.; Benito, A.; Martınez, M.; De La Fuente, G.; Maniette, Y.; Anglaret, E.; Sauvajol, J.-L. Production of high-density single-walled nanotube material by a simple laser-ablation method. *Chem. Phys. Lett.* **1998**, *292*, 587–593.
29. Colomer, J.-F.; Stephan, C.; Lefrant, S.; Van Tendeloo, G.; Willems, I.; Konya, Z.; Fonseca, A.; Laurent, C.; Nagy, J.B. Large-scale synthesis of single-wall carbon nanotubes by catalytic chemical vapor deposition (CCVD) method. *Chem. Phys. Lett.* **2000**, *317*, 83–89. [CrossRef]
30. Kong, J.; Cassell, A.M.; Dai, H. Chemical vapor deposition of methane for single-walled carbon nanotubes. *Chem. Phys. Lett.* **1998**, *292*, 567–574. [CrossRef]
31. Cassell, A.M.; Raymakers, J.A.; Kong, J.; Dai, H. Large scale CVD synthesis of single-walled carbon nanotubes. *J. Phys. Chem. B* **1999**, *103*, 6484–6492. [CrossRef]
32. Kong, J.; Soh, H.T.; Cassell, A.M.; Quate, C.F.; Dai, H. Synthesis of individual single-walled carbon nanotubes on patterned silicon wafers. *Nature* **1998**, *395*, 878–881. [CrossRef]
33. Lamura, G.; Andreone, A.; Yang, Y.; Barbara, P.; Vigolo, B.; Hérold, C.; Marêché, J.-F.; Lagrange, P.; Cazayous, M.; Sacuto, A. High-crystalline single-and double-walled carbon nanotube mats grown by chemical vapor deposition. *J. Phys. Chem. C* **2007**, *111*, 15154–15159. [CrossRef]
34. José-Yacamán, M.; Miki-Yoshida, M.; Rendon, L.; Santiesteban, J. Catalytic growth of carbon microtubules with fullerene structure. *Appl. Phys. Lett.* **1993**, *62*, 657–659. [CrossRef]
35. Ivanov, V.; Nagy, J.; Lambin, P.; Lucas, A.; Zhang, X.; Zhang, X.; Bernaerts, D.; Van Tendeloo, G.; Amelinckx, S.; Van Landuyt, J. The study of carbon nanotubules produced by catalytic method. *Chem. Phys. Lett.* **1994**, *223*, 329–335. [CrossRef]
36. Camilli, L.; Scarselli, M.; Del Gobbo, S.; Castrucci, P.; Nanni, F.; Gautron, E.; Lefrant, S.; De Crescenzi, M. The synthesis and characterization of carbon nanotubes grown by chemical vapor deposition using a stainless steel catalyst. *Carbon* **2011**, *49*, 3307–3315. [CrossRef]
37. Takagi, D.; Hibino, H.; Suzuki, S.; Kobayashi, Y.; Homma, Y. Carbon Nanotube Growth from Semiconductor Nanoparticles. *Nano Lett.* **2007**, *7*, 2272–2275. [CrossRef] [PubMed]
38. Capasso, A.; Waclawik, E.; Bell, J.M.; Ruffell, S.; Sgarlata, A.; Scarselli, M.; De Crescenzi, M.; Motta, N. Carbon nanotube synthesis from germanium nanoparticles on patterned substrates. *J. Non-Cryst. Solids* **2010**, *356*, 1972–1975. [CrossRef]
39. Coleman, J.N.; Khan, U.; Blau, W.J.; Gun'ko, Y.K. Small but strong: A review of the mechanical properties of carbon nanotube–polymer composites. *Carbon* **2006**, *44*, 1624–1652. [CrossRef]
40. Thostenson, E.T.; Ren, Z.; Chou, T.-W. Advances in the science and technology of carbon nanotubes and their composites: A review. *Compos. Sci. Technol.* **2001**, *61*, 1899–1912. [CrossRef]
41. Tans, S.J.; Verschueren, A.R.; Dekker, C. Room-temperature transistor based on a single carbon nanotube. *Nature* **1998**, *393*, 49–52. [CrossRef]
42. Park, S.; Vosguerichian, M.; Bao, Z. A review of fabrication and applications of carbon nanotube film-based flexible electronics. *Nanoscale* **2013**, *5*, 1727–1752. [CrossRef] [PubMed]
43. Wang, C.; Zhang, J.; Ryu, K.; Badmaev, A.; De Arco, L.G.; Zhou, C. Wafer-scale fabrication of separated carbon nanotube thin-film transistors for display applications. *Nano Lett.* **2009**, *9*, 4285–4291. [CrossRef] [PubMed]
44. Passacantando, M.; Bussolotti, F.; Grossi, V.; Santucci, S.; Ambrosio, A.; Ambrosio, M.; Ambrosone, G.; Carillo, V.; Coscia, U.; Maddalena, P. Photoconductivity in defective carbon nanotube sheets under ultraviolet–visible–near infrared radiation. *Appl. Phys. Lett.* **2008**, *93*, 051911. [CrossRef]
45. Castrucci, P.; Scilletta, C.; Del Gobbo, S.; Scarselli, M.; Camilli, L.; Simeoni, M.; Delley, B.; Continenza, A.; De Crescenzi, M. Light harvesting with multiwall carbon nanotube/silicon heterojunctions. *Nanotechnology* **2011**, *22*, 115701. [CrossRef] [PubMed]
46. Del Gobbo, S.; Castrucci, P.; Scarselli, M.; Camilli, L.; De Crescenzi, M.; Mariucci, L.; Valletta, A.; Minotti, A.; Fortunato, G. Carbon nanotube semitransparent electrodes for amorphous silicon based photovoltaic devices. *Appl. Phys. Lett.* **2011**, *98*, 183113. [CrossRef]
47. Reddy, A.L.M.; Shaijumon, M.M.; Gowda, S.R.; Ajayan, P.M. Coaxial MnO_2/carbon nanotube array electrodes for high-performance lithium batteries. *Nano Lett.* **2009**, *9*, 1002–1006. [CrossRef] [PubMed]
48. Zhou, G.; Wang, D.-W.; Li, F.; Hou, P.-X.; Yin, L.; Liu, C.; Lu, G.Q.M.; Gentle, I.R.; Cheng, H.-M. A flexible nanostructured sulphur–carbon nanotube cathode with high rate performance for Li-S batteries. *Energy Environ. Sci.* **2012**, *5*, 8901–8906. [CrossRef]

49. An, K.H.; Kim, W.S.; Park, Y.S.; Moon, J.M.; Bae, D.J.; Lim, S.C.; Lee, Y.S.; Lee, Y.H. Electrochemical properties of high-power supercapacitors using single-walled carbon nanotube electrodes. *Adv. Funct. Mater.* **2001**, *11*, 387–392. [CrossRef]
50. Shimizu, Y.; Egashira, M. Basic Aspects and Challenges of Semiconductor Gas Sensors. *MRS Bull.* **2013**, *24*, 18–24. [CrossRef]
51. Collins, P.G.; Bradley, K.; Ishigami, M.; Zettl, D.A. Extreme oxygen sensitivity of electronic properties of carbon nanotubes. *Science* **2000**, *287*, 1801–1804. [CrossRef]
52. Huang, C.; Huang, B.; Jang, Y.; Tsai, M.; Yeh, C. Three-terminal CNTs gas sensor for N_2 detection. *Diam. Relat. Mater.* **2005**, *14*, 1872–1875. [CrossRef]
53. Evans, G.P.; Buckley, D.J.; Adedigba, A.-L.; Sankar, G.; Skipper, N.T.; Parkin, I.P. Controlling the Cross-Sensitivity of Carbon Nanotube-Based Gas Sensors to Water Using Zeolites. *ACS Appl. Mater. Interfaces* **2016**, *8*, 28096–28104. [CrossRef] [PubMed]
54. Ding, D.; Chen, Z.; Rajaputra, S.; Singh, V. Hydrogen sensors based on aligned carbon nanotubes in an anodic aluminum oxide template with palladium as a top electrode. *Sens. Actuators B Chem.* **2007**, *124*, 12–17. [CrossRef]
55. Penza, M.; Rossi, R.; Alvisi, M.; Serra, E. Metal-modified and vertically aligned carbon nanotube sensors array for landfill gas monitoring applications. *Nanotechnology* **2010**, *21*, 105501. [CrossRef] [PubMed]
56. Kauffman, D.R.; Sorescu, D.C.; Schofield, D.P.; Allen, B.L.; Jordan, K.D.; Star, A. Understanding the sensor response of metal-decorated carbon nanotubes. *Nano Lett.* **2010**, *10*, 958–963. [CrossRef]
57. Leghrib, R.; Felten, A.; Demoisson, F.; Reniers, F.; Pireaux, J.-J.; Llobet, E. Room-temperature, selective detection of benzene at trace levels using plasma-treated metal-decorated multiwalled carbon nanotubes. *Carbon* **2010**, *48*, 3477–3484. [CrossRef]
58. Abdelhalim, A.; Winkler, M.; Loghin, F.; Zeiser, C.; Lugli, P.; Abdellah, A. Highly sensitive and selective carbon nanotube-based gas sensor arrays functionalized with different metallic nanoparticles. *Sens. Actuators B Chem.* **2015**, *220*, 1288–1296. [CrossRef]
59. Wei, B.-Y.; Hsu, M.-C.; Su, P.-G.; Lin, H.-M.; Wu, R.-J.; Lai, H.-J. A novel SnO_2 gas sensor doped with carbon nanotubes operating at room temperature. *Sens. Actuators B Chem.* **2004**, *101*, 81–89. [CrossRef]
60. Espinosa, E.; Ionescu, R.; Chambon, B.; Bedis, G.; Sotter, E.; Bittencourt, C.; Felten, A.; Pireaux, J.-J.; Correig, X.; Llobet, E. Hybrid metal oxide and multiwall carbon nanotube films for low temperature gas sensing. *Sens. Actuators B Chem.* **2007**, *127*, 137–142. [CrossRef]
61. Nguyet, Q.T.M.; Duy, N.V.; Hung, C.M.; Hoa, N.D.; Hieu, N.V. Ultrasensitive NO_2 gas sensors using hybrid heterojunctions of multi-walled carbon nanotubes and on-chip grown SnO_2 nanowires. *Appl. Phys. Lett.* **2018**, *112*, 153110. [CrossRef]
62. Yang, N.; Chen, X.; Ren, T.; Zhang, P.; Yang, D. Carbon nanotube based biosensors. *Sens. Actuators B Chem.* **2015**, *207*, 690–715. [CrossRef]
63. Patolsky, F.; Zheng, G.; Hayden, O.; Lakadamyali, M.; Zhuang, X.; Lieber, C.M. Electrical detection of single viruses. *Proc. Natl. Acad. Sci. USA* **2004**, *101*, 14017–14022. [CrossRef]
64. Star, A.; Gabriel, J.-C.P.; Bradley, K.; Grüner, G. Electronic Detection of Specific Protein Binding Using Nanotube FET Devices. *Nano Lett.* **2003**, *3*, 459–463. [CrossRef]
65. Villamizar, R.A.; Maroto, A.; Rius, F.X.; Inza, I.; Figueras, M.J. Fast detection of Salmonella Infantis with carbon nanotube field effect transistors. *Biosens. Bioelectron.* **2008**, *24*, 279–283. [CrossRef] [PubMed]
66. Star, A.; Joshi, V.; Han, T.-R.; Altoé, M.V.P.; Grüner, G.; Stoddart, J.F. Electronic Detection of the Enzymatic Degradation of Starch. *Org. Lett.* **2004**, *6*, 2089–2092. [CrossRef] [PubMed]
67. Sharf, T.; Kevek, J.W.; DeBorde, T.; Wardini, J.L.; Minot, E.D. Origins of Charge Noise in Carbon Nanotube Field-Effect Transistor Biosensors. *Nano Lett.* **2012**, *12*, 6380–6384. [CrossRef] [PubMed]
68. Lee, J.U.; Gipp, P.P.; Heller, C.M. Carbon nanotube p-n junction diodes. *Appl. Phys. Lett.* **2004**, *85*, 145–147. [CrossRef]
69. Lee, J.U. Photovoltaic effect in ideal carbon nanotube diodes. *Appl. Phys. Lett.* **2005**, *87*, 073101. [CrossRef]
70. Zhou, C.; Kong, J.; Yenilmez, E.; Dai, H. Modulated Chemical Doping of Individual Carbon Nanotubes. *Science* **2000**, *290*, 1552–1555. [CrossRef]
71. Chen, H.; Xi, N.; Lai, K.W.C. Chapter 7—Carbon Nanotube Schottky Photodiodes. In *Nano Optoelectronic Sensors and Devices*; Xi, N., Lai, K.W.C., Eds.; William Andrew Publishing: Oxford, UK, 2012; pp. 107–123.

72. Yang, L.; Wang, S.; Zeng, Q.; Zhang, Z.; Pei, T.; Li, Y.; Peng, L.-M. Efficient photovoltage multiplication in carbon nanotubes. *Nat. Photonics* **2011**, *5*, 672–676. [CrossRef]
73. Merchant, C.; Marković, N. The photoresponse of spray-coated and free-standing carbon nanotube films with Schottky contacts. *Nanotechnology* **2009**, *20*, 175202. [CrossRef] [PubMed]
74. Liu, Y.; Wei, N.; Zeng, Q.; Han, J.; Huang, H.; Zhong, D.; Wang, F.; Ding, L.; Xia, J.; Xu, H. Room temperature broadband infrared carbon nanotube photodetector with high detectivity and stability. *Adv. Opt. Mater.* **2016**, *4*, 238–245. [CrossRef]
75. Itkis, M.E.; Borondics, F.; Yu, A.; Haddon, R.C. Bolometric Infrared Photoresponse of Suspended Single-Walled Carbon Nanotube Films. *Science* **2006**, *312*, 413–416. [CrossRef] [PubMed]
76. Rogalski, A. Infrared detectors: Status and trends. *Prog. Quantum Electron.* **2003**, *27*, 59–210. [CrossRef]
77. Xu, S.; Chua, S.; Mei, T.; Wang, X.; Zhang, X.; Karunasiri, G.; Fan, W.; Wang, C.; Jiang, J.; Wang, S. Characteristics of InGaAs quantum dot infrared photodetectors. *Appl. Phys. Lett.* **1998**, *73*, 3153–3155. [CrossRef]
78. Jiang, J.; Mi, K.; Tsao, S.; Zhang, W.; Lim, H.; O'sullivan, T.; Sills, T.; Razeghi, M.; Brown, G.; Tidrow, M. Demonstration of a 256 × 256 middle-wavelength infrared focal plane array based on InGaAs/InGaP quantum dot infrared photodetectors. *Appl. Phys. Lett.* **2004**, *84*, 2232–2234. [CrossRef]
79. Aramo, C.; Ambrosio, M.; Bonavolontà, C.; Boscardin, M.; Crivellari, M.; de Lisio, C.; Grossi, V.; Maddalena, P.; Passacantando, M.; Valentino, M. Large area CNT-Si heterojunction for photodetection. *Nucl. Instrum. Methods Phys. Res. Sect. A* **2017**, *845*, 12–15. [CrossRef]
80. Liu, L.; Zhang, Y. Multi-wall carbon nanotube as a new infrared detected material. *Sens. Actuators A Phys.* **2004**, *116*, 394–397. [CrossRef]
81. Afrin, R.; Khaliq, J.; Islam, M.; Gul, I.H.; Bhatti, A.S.; Manzoor, U. Synthesis of multiwalled carbon nanotube-based infrared radiation detector. *Sens. Actuators A Phys.* **2012**, *187*, 73–78. [CrossRef]
82. Li, X.; Jia, Y.; Cao, A. Tailored single-walled carbon nanotube− CdS nanoparticle hybrids for tunable optoelectronic devices. *ACS Nano* **2009**, *4*, 506–512. [CrossRef]
83. Kongkanand, A.; Martínez Domínguez, R.; Kamat, P.V. Single Wall Carbon Nanotube Scaffolds for Photoelectrochemical Solar Cells. Capture and Transport of Photogenerated Electrons. *Nano Lett.* **2007**, *7*, 676–680. [CrossRef] [PubMed]
84. Scarselli, M.; Camilli, L.; Matthes, L.; Pulci, O.; Castrucci, P.; Gatto, E.; Venanzi, M.; Crescenzi, M.D. Photoresponse from noble metal nanoparticles-multi walled carbon nanotube composites. *Appl. Phys. Lett.* **2012**, *101*, 241113. [CrossRef]
85. Zhou, C.; Wang, S.; Sun, J.; Wei, N.; Yang, L.; Zhang, Z.; Liao, J.; Peng, L.-M. Plasmonic enhancement of photocurrent in carbon nanotube by Au nanoparticles. *Appl. Phys. Lett.* **2013**, *102*, 103102. [CrossRef]
86. Salvetat, J.-P.; Bonard, J.-M.; Thomson, N.; Kulik, A.; Forro, L.; Benoit, W.; Zuppiroli, L. Mechanical properties of carbon nanotubes. *Appl. Phys. A* **1999**, *69*, 255–260. [CrossRef]
87. Ebbesen, T.; Lezec, H.; Hiura, H.; Bennett, J.; Ghaemi, H.; Thio, T. Electrical conductivity of individual carbon nanotubes. *Nature* **1996**, *382*, 54–56. [CrossRef]
88. Gerlach, C.; Krumm, D.; Illing, M.; Lange, J.; Kanoun, O.; Odenwald, S.; Hübler, A. Printed MWCNT-PDMS-composite pressure sensor system for plantar pressure monitoring in ulcer prevention. *IEEE Sens. J.* **2015**, *15*, 3647–3656. [CrossRef]
89. Park, J.; Lee, Y.; Hong, J.; Ha, M.; Jung, Y.-D.; Lim, H.; Kim, S.Y.; Ko, H. Giant Tunneling Piezoresistance of Composite Elastomers with Interlocked Microdome Arrays for Ultrasensitive and Multimodal Electronic Skins. *ACS Nano* **2014**, *8*, 4689–4697. [CrossRef]
90. Nela, L.; Tang, J.; Cao, Q.; Tulevski, G.; Han, S.-J. Large-Area High-Performance Flexible Pressure Sensor with Carbon Nanotube Active Matrix for Electronic Skin. *Nano Lett.* **2018**, *18*, 2054–2059. [CrossRef]
91. Gui, X.; Wei, J.; Wang, K.; Cao, A.; Zhu, H.; Jia, Y.; Shu, Q.; Wu, D. Carbon nanotube sponges. *Adv. Mater.* **2010**, *22*, 617–621. [CrossRef]
92. Novikov, S.; Lebedeva, N.; Satrapinski, A.; Walden, J.; Davydov, V.; Lebedev, A. Graphene based sensor for environmental monitoring of NO_2. *Sens. Actuators B Chem.* **2016**, *236*, 1054–1060. [CrossRef]
93. Helland, A.; Wick, P.; Koehler, A.; Schmid, K.; Som, C. Reviewing the environmental and human health knowledge base of carbon nanotubes. *Environ. Health Perspect.* **2007**, *115*, 1125–1131. [CrossRef]

94. Pacurari, M.; Castranova, V.; Vallyathan, V. Single-and multi-wall carbon nanotubes versus asbestos: Are the carbon nanotubes a new health risk to humans? *J. Toxicol. Environ. Health Part A* **2010**, *73*, 378–395. [CrossRef] [PubMed]
95. Yang, L.; Wang, S.; Zeng, Q.; Zhang, Z.; Peng, L.-M. Carbon Nanotube Photoelectronic and Photovoltaic Devices and their Applications in Infrared Detection. *Small* **2013**, *9*, 1225–1236. [CrossRef] [PubMed]
96. Hou, P.-X.; Liu, C.; Cheng, H.-M. Purification of carbon nanotubes. *Carbon* **2008**, *46*, 2003–2025. [CrossRef]
97. Geier, M.L.; McMorrow, J.J.; Xu, W.; Zhu, J.; Kim, C.H.; Marks, T.J.; Hersam, M.C. Solution-processed carbon nanotube thin-film complementary static random access memory. *Nat. Nanotechnol.* **2015**, *10*, 944–948. [CrossRef] [PubMed]
98. Brady, G.J.; Joo, Y.; Wu, M.-Y.; Shea, M.J.; Gopalan, P.; Arnold, M.S. Polyfluorene-Sorted, Carbon Nanotube Array Field-Effect Transistors with Increased Current Density and High On/Off Ratio. *ACS Nano* **2014**, *8*, 11614–11621. [CrossRef]
99. Si, J.; Zhong, D.; Xu, H.; Xiao, M.; Yu, C.; Zhang, Z.; Peng, L.-M. Scalable Preparation of High-Density Semiconducting Carbon Nanotube Arrays for High-Performance Field-Effect Transistors. *ACS Nano* **2018**, *12*, 627–634. [CrossRef]
100. De Volder, M.F.L.; Tawfick, S.H.; Baughman, R.H.; Hart, A.J. Carbon Nanotubes: Present and Future Commercial Applications. *Science* **2013**, *339*, 535–539. [CrossRef]